Modeling the Urban Heat Island in Gothenburg, Sweden: an analysis of the Urban Weather Generator

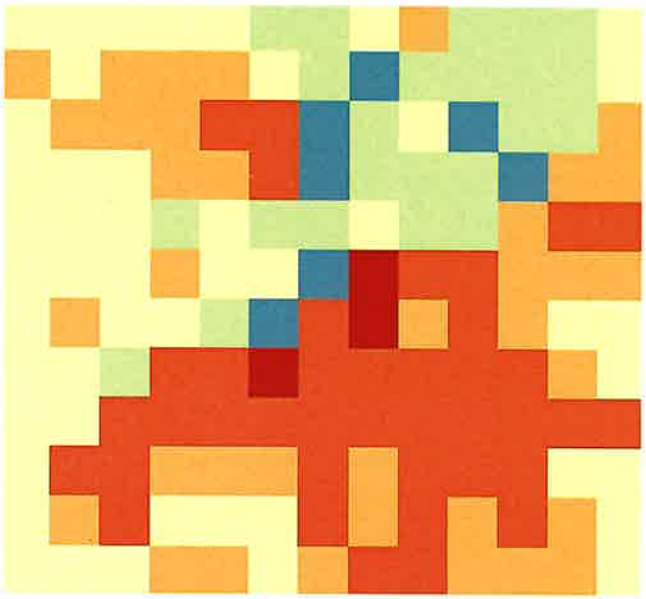

Louise Lindén

Degree of Master of Science (120 credits)
with a major in Geography
30 hec

Department of Earth Sciences
University of Gothenburg
2023 B1209

Faculty of Science

UNIVERSITY OF GOTHENBURG

UNIVERSITY OF GOTHENBURG
Department of Earth Sciences
Geovetarcentrum/Earth Science Centre

Modeling the Urban Heat Island in Gothenburg, Sweden: an analysis of the Urban Weather Generator

Louise Lindén

ISSN 1400-3821

B1209
Master of Science (120 credits) thesis
Göteborg 2023

Mailing address
Geovetarcentrum
S 405 30 Göteborg

Address
Geovetarcentrum
Guldhedsgatan 5A

Telephone
031-786 19 56

Geovetarcentrum
Göteborg University
S-405 30 Göteborg
SWEDEN

Abstract

Urban Heat Islands is a well-known phenomenon that has been observed in most cities around the globe. It is a night-time phenomenon occurring on calm and clear nights and is defined as the temperature difference between an urban area and its rural surroundings. As air temperatures are getting higher due to climate change, along with a global trend of urbanization, there is a need to identify the risks of urban heat to implement heat-mitigating measures. One method for modeling Urban Heat Islands is the Urban Weather Generator (UWG). This study aims to investigate the characteristics of the UWG and evaluate how well it performs in the city of Gothenburg, Sweden. A sensitivity analysis of the different input parameters was performed, as well as a model evaluation where modeled data was compared to observed air temperatures from five different sites around Gothenburg. Building density is the parameter that most influenced the modeled air temperatures, while vegetation had a low effect on the modeled results. The results of the model evaluation showed that the model estimates urban air temperatures well in built-up dense areas, while areas with a high fraction of vegetation were not captured efficiently by the model. In these areas, the modeled air temperature was higher than the observed. Therefore, one can conclude that the model performs well in estimating air temperatures in typical urban environments, while it needs improvements in capturing the mitigating effects of urban vegetation.

Keywords: urban climate, urban heat island, Urban Weather Generator, urban planning

Acknowledges

This thesis is the result of the 2-year master's program in Geography at the University of Gothenburg.

A huge thank you goes out to my supervisors, Fredrik Lindberg and Jérémy Bernard, for all your much-needed advice and encouragement throughout this process. Also, I would like to thank my classmates in the Geography master's program. Although two years of Zoom lectures and meetings have been challenging, we could still find support amongst each other.

I would also like to thank Norconsult AB, who has given me an office to go to (much needed after two years of studying from home) and colleagues to enjoy coffee breaks with. A special thanks to Sara Holmström and Sonja Sandström, who has given me lots of valuable input and support, both when it comes to writing and GIS. Also, thanks to Mikaela for always being a supportive office neighbor as we were both writing and (sometimes) struggling with our master theses.

Last but not least, I would like to express my deepest gratitude to my friends and family who have supported me along the way.

Louise Lindén
May 2022

Table of Contents

1 Introduction

1.1 Background

Most people can probably relate to the feeling of wanting to escape the unbearable heat of the city on a hot summer day, perhaps seeking relief in the countryside or by the coast. In fact, most urban areas experience higher air temperatures than rural. The average temperature difference is about 1-3 °C higher in urban areas, but this difference can be up to 12 °C in large cities under certain weather conditions (Grimmond, 2007; Oke et al., 2017). This phenomenon is called the Urban Heat Island (UHI) and has been observed in many cities around the world. The UHI is defined as the difference in temperature between an urban area and its rural surroundings. The differential cooling rates of the urban and rural sites during the evening and early night cause this temperature difference, making the UHI a nocturnal phenomenon (Oke et al., 2017). The UHI forms due to a combination of circumstances, mainly the urban geometry, lack of vegetation, meteorological factors, anthropogenic heat release, and the urban materials affecting the thermal admittance (Santamouris et al., 2017).

According to The Intergovernmental Panel on Climate Change (IPCC), it is virtually certain (more than 99% probability) that the extensive release of greenhouse gases already has caused an increase in mean air temperatures as well as extreme heatwaves in most parts of the world, a trend that will continue over the 21st century (IPCC, 2021). The UHI has been identified as intensifying the heat extremes in urban areas (IPCC, 2021). The increase in urban temperatures has been shown to increase mortality and morbidity, especially in vulnerable groups such as old adults (Mirzaei et al., 2012; Santamouris et al., 2017). With the UHI being more distinct during the night, nighttime recovery is harder during heat waves, and the risk for heat stress-related diseases and mortality increases for people in the city, especially among the most vulnerable groups (Fischer et al., 2012). The UHI can increase a building's cooling need by up to 100%, and in combination with other factors, such as climate change and a growing urban population, the cooling demands will increase significantly globally over the coming years (Santamouris et al., 2017). In Sweden, not many dwellings have air-conditioning, since it has not been necessary due to the mild climate. Nevertheless, with a more urbanized population living in dense cities, along with higher mean air temperatures and the high risk of more intense and frequent extreme heat events,

the demand for heat-mitigating measures will increase even in countries such as Sweden (IPCC, 2021; Thorsson et al., 2011). Therefore, there is a need to locate the largest magnitudes of the UHI, in order to identify the people at risk of heat stress, as well as locate the largest needs for cooling measures.

Measuring the magnitude of the UHI is usually challenging, as it requires a comprehensive use of observational stations measuring air temperatures for a long period of time (Hardin et al., 2018). Since the urban characteristics vary within the city, there will be intra-urban differences of the UHI. Therefore, only one or a few observational stations are not enough to capture the variations of the city (Smoliak et al., 2015). Thus, a well-functioning model to predict air temperatures would significantly help examine the UHI. In 2013, Bueno et al. proposed a new model that predicts the UHI on a local scale, the Urban Weather Generator (UWG). Since then, the model has been evaluated for cities such as Basel, Toulouse, and Singapore where the modeled data has been compared to observed data with satisfactory results (Bueno et al., 2013, 2014; Yang, 2016). This master thesis presents an evaluation of the UWG in the context of Gothenburg, Sweden.

1.2 Aim

This study aims to investigate the characteristics of the UWG and evaluate how well it performs in the city of Gothenburg, Sweden.

1.3 Research questions

- What parameters influence the UWG and how sensitive is the UWG to changes of these?
- How well does the UWG compare with observed temperature data to predict the UHI?

2 Theoretical background

2.1 The Urban Heat Island

The first acknowledgment of how urban areas affect climate on a local scale dates back to the early 19th century, with observations made by Howard (1833). Since then, the UHI has become a well-known phenomenon and is recognized in most urban areas (Grimmond, 2007). The definition of the UHI as the difference in temperature between an urban and a nearby rural area can be expressed in different ways. The UHI average intensity is the

average UHI over the night, whereas the maximum or minimum UHI is when the difference is the highest or lowest in absolute terms (Hardin et al., 2018).

This section presents the theoretical framework for the different types of UHI: s, the parameters influencing the UHI, and the temporal variations of the UHI. It also presents an introduction to the model evaluated in this study; the Urban Weather Generator (UWG).

2.1.1 Different types of UHI

Four different types of UHI:s are defined by Oke et al. (2017) and presented in TABLE 1. The need for different definitions of the UHI phenomenon is explained by the various heat capacity and rates of heating and cooling between surface, subsurface, and atmosphere in urban and rural areas, respectively (Oke et al., 2017). The UHI in the canopy layer (see TABLE 1), namely the height between the urban ground and the average rooftop/tree height, has the greatest effect on human heat stress and is therefore important to study (van Hove et al., 2015). This study focuses on the Canopy Layer Urban Heat Island, which further in this paper will be referred to as the Urban Heat Island (UHI).

Table 1. Different types of UHI:s as described by Oke et al. (2017).

Types of UHI	***Description***
Urban Canopy Layer Urban Heat Island	*The difference between air temperature in the urban canyon[1], and the equivalent height in the surrounding rural area.*
Boundary Layer Urban Heat Island	*The difference between air temperature in the urban boundary layer, which is the layer defined as the warmer area above the city, influenced by the urban characteristics[2], and the equivalent height in the surrounding rural area.*
Surface Urban Heat Island	*The difference in surface temperature between the urban and rural areas.*
Subsurface Urban Heat Island	*The difference in subsurface temperature of urban and rural areas.*

[1] The micro-scale structure where the street is flanked by urban (tall) buildings, creating a canyon-like environment

[2] Approximately 1-2 km deep during day, while reduced to 100s of meters during night

2.2 Parameters influencing the UHI

Many cities are experiencing an urbanization process, a process which inevitably is accompanied by a drastic change in land cover due to a heavy increase in population; vegetation is replaced by impervious surfaces such as roads and buildings. Consequently, urban areas experience lower rates of evapotranspiration, less reflected solar radiation due to the lower albedo of urban materials like asphalt and concrete, greater heat storage, and less wind as the built-up areas are blocking these (Coutts et al., 2007; Oke et al., 2017). These are all examples of the parameters that influence the formation of a UHI.

The following presented parameters regulating the UHI intensity are a compilation of the *main* findings of different literature, not covering all potential factors. Therefore, the parameters presented here might not be influential in all circumstances or regions. Also, the relationship between these regulating factors is intricate (Grimmond, 2007).

2.2.1 Urban geometry

Urban geometry has a strong connection to the intensity of the UHI (Chow & Roth, 2006; Erell & Williamson, 2007; Holmer et al., 2007; Konarska et al., 2016). This includes the density of the urban buildings, usually measured as the Height-to-Width ratio (H/W ratio), or the sky-view factor (SVF) (Erell & Williamson, 2007). The Height-to-Width ratio is measured as the mean height of the buildings on both sides of a street, divided by the mean width of the street (Lindberg, 2007). The sky-view factor is related to the H/W ratio and is a value between 0-1, in basic terms indicating the fraction of the sky that is observed from the ground. A reduced sky-view factor suggests an obstruction in form of buildings or trees (Konarska et al., 2016).

A lower sky-view factor and/or a higher H/W ratio reduces the emissions of long-wave radiation to the atmosphere (increasing the heat storage), while the daytime absorption of short-wave radiation is also higher due to reflections between the buildings and the street. Therefore, the city provides an overall higher potential for heat absorption due to the many surfaces available (Erell & Williamson, 2007). In a study of intra-urban cooling rates in Gothenburg, Konarska et al., (2016), found the SVF to be the most important factor in slowing down nighttime cooling rates. Similarly, Holmer et al. (2007) found the influence of SVF and heat capacity of buildings as important factors influencing the cooling rates of the first phase of the night in Gothenburg. Besides the uneven warming and cooling of urban

canyons, Lindberg (2007) describes how urban geometry also influences wind speed. The built-up areas are usually blocking the winds and slow them down, whereas in rarer cases, the design of the buildings creates wind tunnels and thereby increases the wind speed (Lindberg, 2007).

2.2.2 Heat storage, thermal properties, and albedo

Other important factors contributing to the UHI are the properties of the materials that are exposed to solar radiation, in terms of their heat storage capacity, permeability, and albedo (Coutts et al., 2007).

The heat storage of cities is larger than in rural areas, and this is mainly restricted to three properties of the urban areas; the thermal properties of the urban materials, access to moisture, and urban geometry (Oke et al., 2017). The urban materials (such as asphalt, concrete, steel et cetera) usually have higher thermal admittance and heat capacity, creating larger heat storage and delayed release of heat compared to vegetation (Oke et al., 2017). A high amount of impervious surfaces, namely surfaces that do not hold water (such as buildings, pavement, and asphalt), will decrease evaporation, leading to less cooling (Kuttler, 2008; Tam et al., 2015). When wet, these surfaces transfer some of the sensible heat into latent heat through evaporation, but this effect is not long-lasting due to the efficient run-off of these surfaces (Kuttler, 2008; Oke, 1982). The soils of the rural areas both infiltrate and evaporate water, and the permeability is higher than that of the urban materials (Oke et al., 2017). However, wet soils have higher thermal admittance than dry, creating a slower nocturnal cooling (Oke et al., 2017), while it contributes to greater evaporative cooling during the day (Konarska et al., 2016). Ramírez-Aguilar and Lucas Souza (2019) found that an area with less than 40 % pervious (vegetated) surfaces, had the largest UHI intensities, indicating the importance of urban greenery.

To compensate for the lack of pervious materials in the city, it is often suggested to instead increase the surface albedo of the urban materials (Erell et al., 2014). Albedo, which is a measure (between 0-1) of a surface's ability to reflect radiation, is potentially a large mitigator of especially surface temperature since it also decreases the absorption of solar radiation (Coutts et al., 2007; Taha, 1997). Light surfaces, such as snow, have a high ability to reflect solar radiation to the atmosphere, while many of the urban surfaces are characterized by darker colors and therefore reflect less of the available radiation (Taha,

1997). Coutts et al. (2007) examined the impact of urban density on the energy balance and found a relationship between the Height-to-Width ratio and larger air canopy temperatures. However, a lower albedo sometimes had a larger effect on the air canopy temperatures than the H/W ratio.

2.2.3 Vegetation

Vegetation influence the UHI both by its shading effects (mainly from trees) and evapotranspiration (evaporation and transpiration), turning sensible heat into latent heat, which is a cooling process (Coutts et al., 2007; Konarska et al., 2016; Tam et al., 2015). In a study of cooling rates of different sites in Gothenburg, Konarska et al. (2016), found that the parks were generally cooler than urban areas, where the greatest temperature difference was found on the hottest days of the summer season. Furthermore, Spronken-Smith & Oke (1998) studied the heating and cooling of parks and found that during daytime, parks with a lot of high trees that shade big areas are often cooler compared to open vegetated areas, such as lawns. This is explained by the fast heating of open spaces, which can be even warmer than their (urban) surroundings (Spronken-Smith & Oke, 1999). However, during nighttime, the effect of high trees in parks is usually reversed, where these parks tend to cool slower than the open areas with low growing vegetation. It is believed that the tree canopies, similar to the urban canyon, block both winds and outgoing longwave radiation (Konarska et al., 2016).

2.2.4 Anthropogenic heat release and population density

Certainly, the city has a higher amount of anthropogenic heat sources, which all contribute to the warmer temperatures of the city (Grimmond, 2007). Sailor and Lu (2004) describe three general types of anthropogenic heat sources; heat from the transportation systems (vehicles); heat from the building sector, which is measured both as electricity consumption and heat from gas or fossil fuels; and heating due to human metabolism. These three contributing factors also have a temporal and spatial variance, such as in the seasonal need for use of warming and cooling of buildings, or the daily patterns of traffic/commuting, which can affect the daily and seasonal variance of the UHI (Sailor & Lu, 2004). Variations of heat release are also seen between different types of building use, such as industrial, commercial, or residential buildings (Tam et al., 2015).

The population density is often highlighted as a contributing factor to more intense UHI:s. However, it can be argued that this effect is rather an indirect effect where the urban geometry and lack of urban greenery is a reflection of the population density, which has been identified by for instance Park (1986) and Ramírez-Aguilar and Lucas Souza (2019). Ramírez-Aguilar and Lucas Souza (2019) compared both (high) SVF and (low amount of) permeable surfaces and these were highly correlated with both high UHI intensities and a high population.

2.2.5 Weather and climate

Nights with clear skies and calm winds most likely experience the most intense UHI:s (Oke et al., 2017). During these circumstances, there is a higher rate of radiative cooling than on cloudy nights (especially in rural and open sites), and the absence of winds leads to a low mixing of air (Oke et al., 2017). Also during the day, clear skies contribute to the UHI, when the urban surfaces are exposed to radiative heating (Grimmond, 2007). Moreover, the volume and thickness of the cloud cover, as well as the type and height of it influences the UHI. A low cloud cover of stratus type would decrease the UHI effect more than thinner clouds at higher altitudes (Morris et al., 2001). Park (1986) observed how high wind speed (above 11.1 m/s) was the main interrupter of UHI intensities in Seoul, South Korea. Above this wind speed, the phenomenon was not found. Morris et al. (2001) found that wind speed above 5 m/s, together with cloud formation, lowered the UHI effect. Several studies have confirmed the influence of the sea breeze (e.g. Salvati et al., 2017; Santamouris et al., 2017). Coastal cities do experience a UHI, but the intensity is decreased by the transportation of cool air from the sea into the city (Santamouris et al., 2017). However, when studying the UHI in Barcelona, Spain, Salvati et al. (2017) found this mitigating effect mainly on the roof-top level in the city, and on the reference rural (airport) site. The sea breeze was not able to decrease the air temperatures at street level, due to the blocking effect of buildings (Salvati et al., 2017).

As already discussed, many studies of cities in temperate climates have confirmed that one of the most influential factors of the UHI is urban geometry. Thus, other factors have been suggested to have a stronger influence on the cooling rates in other types of climates, such as vegetation in hot, semi-arid cities (Konarska et al., 2016). Chow and Roth (2006) studied the UHI in Singapore (tropical hot/dry climate) and did not find the urban structure as the

most influential factor by itself. The authors also argue that a higher H/W ratio does not necessarily increase the canyon heat storage, since it is providing it with shade, decreasing the absorption of incoming solar radiation during the day. Similarly, Ramírez-Aguilar and Lucas Souza (2019) studied the UHI in Bogotá, Colombia (tropical climate) and found the highest UHI intensities for building heights between 4-10 meters while building heights over 13 meters did not increase the urban-rural temperature differences.

2.3 Temporal variations of the UHI

2.3.1 The nighttime urban heat island

In the urban canopy layer, the highest air temperatures are usually reached during the mid or late afternoon (Soltani & Sharifi, 2017; Tam et al., 2015). However, the air temperature difference between the city and its rural surroundings is usually highest during the night, making the UHI a nocturnal phenomenon. The warm air stays longer in the urban structures during late evening and early night, while the radiative cooling is faster in the countryside (Erell & Williamson, 2007; Oke et al., 2017; Soltani & Sharifi, 2017). As suggested by several authors (e.g. Erell & Williamson, 2007; Holmer et al., 2007; Konarska et al., 2016; Onomura et al., 2016), the nocturnal pattern of the UHI can be divided into two main phases. During the first phase, the cooling rates are faster in rural areas where the heat storage is lower than in an urban area, and the outgoing long-wave radiation is not blocked by built-up areas. The cooling rate of the urban site is slower and can be explained by the characteristics of the built-up area, such as the sky-view factor and Height-to-Width ratio, which influences the release of the stored long-wave radiation, which in turn is affected by the urban material's thermal admittance (Chow & Roth, 2006; Erell & Williamson, 2007; Holmer et al., 2007; van Hove et al., 2015). The second phase of the night is characterized by a more even cooling of the urban and rural sites, usually lasting until sunrise, and is not dependent on the site features (Holmer et al., 2007). Haeger-Eugensson & Holmer (1999) suggested that this phase is characterized by the UHI circulation caused by the urban-rural pressure gradient, which enhances the urban cooling rate when the cooler rural air is being fused with the urban air. However, this effect is not always present and does not completely explain the late nocturnal patterns of the UHI (Holmer et al., 2007). Holmer et al. (2007) suggest that this is rather a result of the characteristics of the air layer above the rooftop and therefore the cooling is no longer influenced by the urban geometry in this phase of the night.

The literature on when the UHI intensity is greatest is not consistent, 1-2, 2-3 hours, or 3-5 hours after sunset are suggested (Erell & Williamson, 2007; Kuttler, 2008; Onomura et al., 2016). This varies due to different factors such as climate, size of city and population, and the (urban) attributes of that specific area (Kuttler, 2008; Onomura et al., 2016).

2.3.2 The daytime urban cool island

The daytime proceeding of air temperatures usually, but not always, shows a pattern where urban areas are cooler than the surrounding rural areas. This phenomenon is called the Urban Cool Island (UCI), which is much less researched than the UHI (Erell & Williamson, 2007; Oke et al., 2017). After the second phase of the night, characterized by the even cooling of both urban and rural sites, the sun starts to rise. At this point, the rural areas are usually cooler, but the incoming solar radiation generates fast surface heating in these areas since these are usually more open compared to the shaded urban canyons (Oke et al., 2017). This creates a UCI reaching its maximum around noon or a few hours later (Chow & Roth, 2006; Erell & Williamson, 2007). The intensity of the UCI is usually much weaker than the UHI but typically occurs on sunny and calm days in cities with dense urban geometry and a low proportion of anthropogenic heating (Erell & Williamson, 2007).

2.4 Urban Weather Generator (UWG)

2.4.1 Model description

The Urban Weather Generator (UWG) was originally developed by Bueno et al. (2013) and estimates air temperatures and relative humidity on a local urban scale, based on meteorological data from a nearby rural weather station. The model is based on four components – (i) the Rural Station Model, (ii) Vertical Diffusion Model, (iii) Urban Boundary Layer Model, and (iv) Urban Canopy and Building Energy Model (FIGURE 1). With the input of observed meteorological data from a rural station, The Rural Station Model (i) produces rural sensible heat fluxes which go into the Vertical Diffusion Model (ii). This component uses the rural meteorological data as well as the sensible heat fluxes calculated by the Rural Station Model (i). The Vertical Diffusion Model (ii) computes the vertical potential air temperatures of the rural site, which goes into the Urban Boundary Layer Model (iii) which calculates the air temperatures of the urban boundary layer, differentiated by day and nighttime. This part of the UWG is also provided with data on the urban sensible heat fluxes generated by the Urban Canopy and Building Energy Model (iv). The Building Energy Model incorporated in

this fourth component of the UWG calculates the heat waste of buildings (Bueno et al., 2012). The Urban Canopy and Building Energy Model (iv) calculates the canyon air temperature of the urban area, based on the input meteorological data and the air temperatures of the urban boundary layer calculated by the Urban Boundary Layer Model (Bueno et al., 2013).

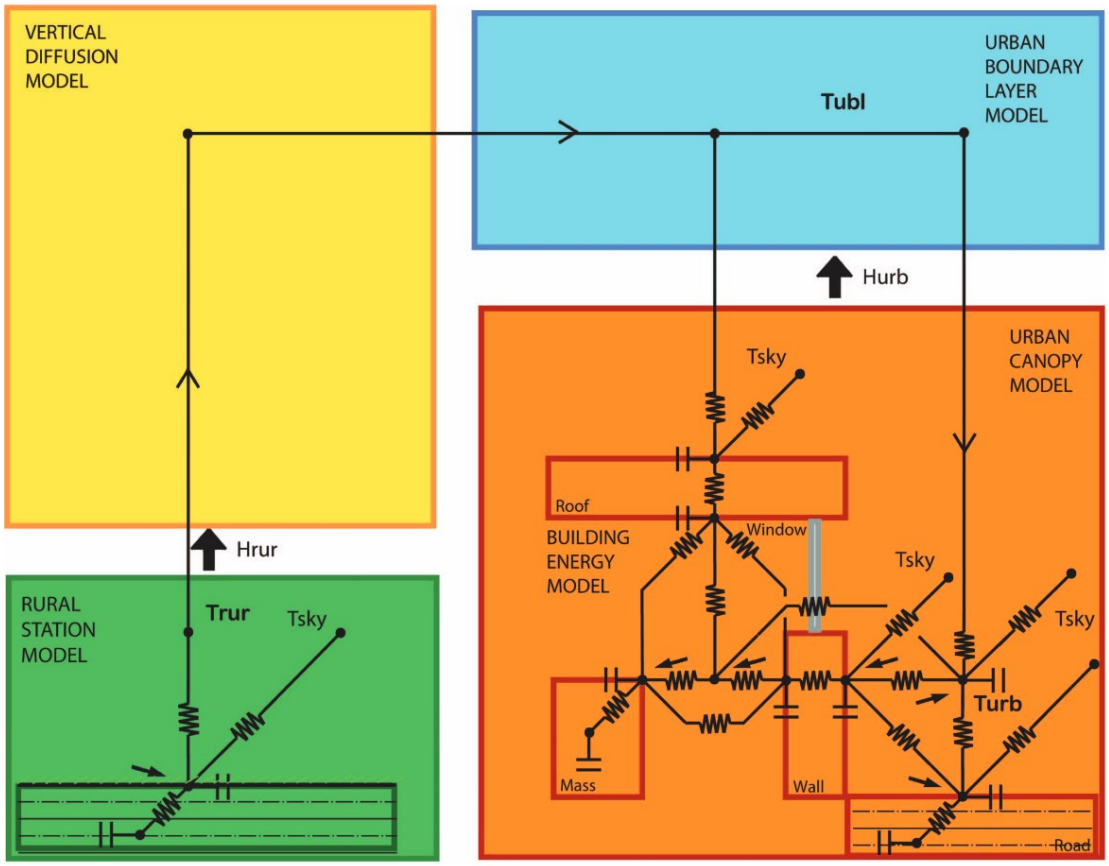

Figure 1. UWG model description, from Bueno et al., (2013)

The model has been improved by Nakano et al. (2015), who identified the key input parameters for the model to simplify the process. Furthermore, Yang (2016) proposed a simplification of the radiative exchanges calculated by the model, as well as introducing an improved Building Energy Model. This new building energy model uses 16 different building types, which can be classified as built before the 80s, after the 80s, or newly constructed. These different building types are accounted for different types of usages (including electrical lighting, hot water use, residency), energy consumption, albedo, and emissivity, amongst other parameters, and are based on typical US building types classified by the US. Department of Energy (Yang, 2016).

More details on the simulations calculated by the UWG model used in this study can be found in Bueno et al. (2013), Nakano et al. (2015), and Yang (2016).

2.4.2 Model Implementation

As input, the UWG requires an EnergyPlus Weather (epw) file of the rural reference station, with hourly data from one year of parameters such as air temperature, relative humidity, air pressure, radiation, and wind (all the required parameters are presented in TABLE 3). The model also makes use of a text file that describes the characteristics of the urban area, such as landcover, morphology (average building height, building density, and wall area), and building types (Nakano et al., 2015). The model output is a new weather file (epw-file) for each grid calculated by the model with altered values of the air temperatures and relative humidity.

For this study, the UWG incorporated in the Urban Multi-Scale Environmental Predictor (UMEP) has been used (Lindberg et al., 2018). UMEP, combining several models and methods, is a tool developed for use in a range of climate-related research, where data can be used for pre-processing, processing, and post-processing. Developed as an open-source tool, it is accessible through QGIS. For this study, the model has been used with QGIS 3.22 version. A flowchart of the UWG model implemented in UMEP is presented in FIGURE 2.

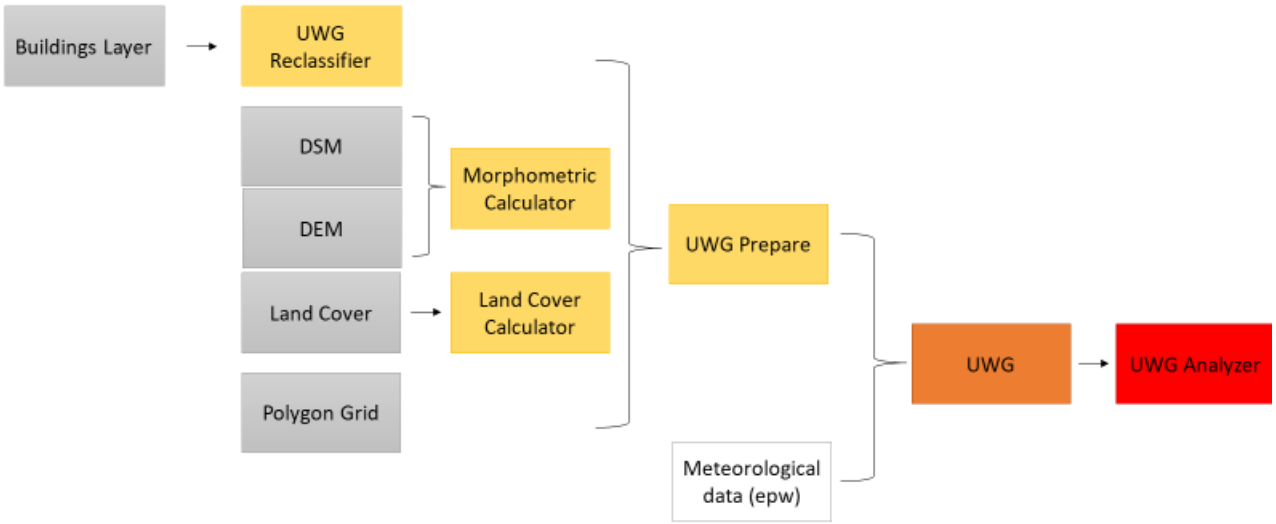

Figure 2. Flowchart of the UWG model and input data used in this study. The grey boxes represent input geodatasets, and the white boxes represent other types of input data. The yellow, orange, and red boxes represent the pre-processor, processor, and post-processor plugins in UMEP, respectively.

As already mentioned, the UWG requires an epw-file and a text file as input. For this study, the text file was prepared using three pre-processing tools incorporated in UMEP (Lindberg et al., 2018);

1. *Morphometric Calculator (grid)* – using a DEM and a DSM, this tool calculates the morphometric parameters (building height, building density, Vertical to Horizontal) required for the UWG.
2. *Land Cover Fraction (grid)* – calculates the land cover fraction of each grid. For this study, an already classified Land Cover raster layer has been used, otherwise, this can be prepared using the "Land Cover Reclassifier"-plugin in UMEP.
3. *UWG Reclassifier* – reclassifies buildings into UWG format. Requires a vector layer of building types on a neighborhood scale. This parameter is optional and if not applied, all buildings are set to "Mid-rise Apartment" by default.

These three parameters, together with a polygon grid layer (which can be prepared in any GIS program), are then used in the "UWG Prepare" to create the text file required for the UWG. In this plugin, the climate zone of the study area is also set, where there are 16 different climate zones available.

All the simulations run by the UWG in this study were set to a simulation time step of 150 seconds, except for the Slottsskogen area (more information on the different study sites is found in section **3.4**) which was run with a simulation step of 100 seconds. The climate zone for Gothenburg was set to 4C (Mild; Marine).

3 Method

This study is using a quantitative method on assessing how well the UWG predicts the UHI in the city of Gothenburg and what parameters influence the model. The UWG requires meteorological data of a rural site, as well as ground cover and morphological information, and optionally, a layer of building classifications. All data has been processed by the Urban Weather Generator (UWG) where a sensitivity analysis and a model evaluation have been carried out. The following section presents an introduction of the study area, along with a description of the data used in this study and how this has been collected, processed, and analyzed.

3.1 Study area

The area of interest for this study is the city of Gothenburg (57°42'N, 11°58'E), Sweden's second-largest city located on the west coast of the country (FIGURE 3). The city was inhabited by about 588 000 people by the end of 2021 (Statistiska Centralbyrån, 2022). The population is expected to grow by about 120 000 people by 2040, with some uncertainties regarding immigration and domestic movements, where the covid-19 pandemic will or already has been affecting the moving patterns (Stadsledningskontoret, 2022). The built-up areas of the central parts of the city have a typically old European structure and are characterized by mid-rise, dense buildings, narrow streets, and a low fraction of vegetation (Konarska et al., 2016; Thorsson et al., 2011). There are some urban parks, but more vegetation is found further out from the city center. With the expected increase of inhabitants in the city there is a pronounced goal from local politicians to densify the city. The plan from the authorities is to constrain the urban sprawl to concentrate development in the already urbanized areas (Vilhelmson & Elldér, 2021). This type of development has already been seen in some of the central parts, for instance in "Nya Kvillebäcken", where the built-up area is characterized by its densely placed high-rise apartment buildings and a low fraction of vegetation.

3.1.1 Climate of Gothenburg

Gothenburg is a high-altitude city with a temperate, marine climate (Konarska et al., 2016; Thorsson et al., 2011). The length of the day varies around the year, from about 6 h in the winter and 18 h in the summer (Konarska et al., 2016). The annual average temperature is 8.9 °C, while the average air temperature for winter (December to February) is 1.2 °C and 17.2 °C for summer (June to August), based on temperature measurements between 1991-2020 (SMHI, n.d.). The annual average air temperatures have increased by 1.4 °C, compared to the period of 1961-1990 when the annual mean air temperature was 7.5 °C (SMHI, n.d.).

3.2 Data collection

This section presents the different types of data used for this study, which have been distinguished as geospatial ground data, meteorological data, and observed data.

3.2.1 Geospatial ground data

An overview of the geospatial datasets used in this study is presented in TABLE 2**.**

The UWG requires indicators of urban morphology which in this study have been calculated from three sets of raster ground data: a Digital Elevation Model (DEM), a Digital Surface Model (DSM), and a set of Land Cover data. The DEM represents the bare surface, without vegetation and buildings, while these are included in the DSM. The Land Cover raster layer is based on LiDAR data processed by Johansson (2018) and divided into seven classes; water, buildings, paved, bare soils, grass, deciduous, and evergreen trees. More information on how this layer was processed is found in Johansson (2018).

A vector layer, consisting of building types is also used as input to the model. For this study, this layer is based on a vector layer "Urban Typology" (Bäcklin, 2020) consisting of building types that are found in Gothenburg, which was merged with data from the Urban Atlas (2018) to cover the parts that are not classified in the "Urban Typology" layer. These were then classified accordingly to the 16 classes found in the UWG, and in this case study, the main classification types used were "Mid-rise Apartment" and "Warehouse".

Table 2. Geospatial datasets used for this study.

Dataset	Resolution	Source	Information/modifications	Application
DSM, Digital Surface Model	1 m	The City of Gothenburg (2010).	This layer was merged with an updated DSM of "Kvillebäcken" from 2018.	Morphological calculations to use as input in the UWG.
DEM, Digital Elevation Model	1 m	The City of Gothenburg (2010).		Morphological calculations to use as input in the UWG.
Land Cover	1 m	Johansson (2018).	Raster layer consisting of 7 types of ground cover; water, buildings, paved, bare soils, grass, deciduous, and evergreen trees.	Calculating Land cover fractions to use as input in the UWG.
Urban Atlas 2018	Vector data	Copernicus Land Monitoring Service (2018).	Merged with the values of the dataset "Urban Typology".	Input in the UWG.
Urban typology	Vector data	Oskar Bäcklin, PhD Student at University of Gothenburg (2020).	Vector layer with polygons representing different building types on a neighborhood scale.	Input in the UWG.
Polygon grid layer of central Gothenburg	500x500 m (squares)	Prepared in QGIS.		Input in the UWG.
Polygon grid layer of 5 weather stations	100 m radius (circles)	Prepared in QGIS.		Input in the UWG.

3.2.2 Meteorological data

To generate urban air temperatures, the UWG makes use of yearly meteorological data from an adjacent rural station, as presented in TABLE 3**.** All data was gathered for the year 2021. The UWG model uses an EnergyPlus Weather (epw) file format when running, thus the values of TABLE 3 were converted into this file format. Data needing processing and/or calculations are presented below TABLE 3.

Table 3. Meteorological data for 2021, used as input for the UWG model.

Type of data	**Source**	**m above sea level**	**Temporal resolution**	**Unit**	**UTC**
Air temperature	SMHI Landvetter station (SMHI, 2021)	154	Hourly	°C	0
Dewpoint temperature	Calculated based on SMHI data (2021)			°C	0
Relative Humidity	SMHI Landvetter station (SMHI, 2021)	154	Hourly	%	0
Air pressure	GVC station	72	10-minute	Pa	+1
Longwave radiation - L_{down}	GVC station	72	10-minute	w/m^2	+1
Global shortwave radiation - K_{down}	GVC station	72	10-minute	w/m^2	+1
Direct shortwave radiation - K_{dir}	Calculated based on GVC data			w/m^2	+1
Diffuse shortwave radiation - K_{diff}	GVC station	72	10-minute	w/m^2	+1
Wind direction - W_{dir}	GVC station	72	10-minute	°	+1
Wind speed - W_s	GVC station	72	10-minute	m/s	+1
Soil temperature	Muñoz Sabater (2021)		Hourly	°C	0

The Landvetter station is used as the rural reference station that the UWG uses to produce urban air temperatures. This data is provided by the Swedish Meteorological and Hydrological Institute (SMHI, 2021) and is observed on an hourly basis. The weather station is placed close to the Landvetter Airport, which is located in Härryda municipality, approximately 20 km east of Gothenburg. The station on Landvetter Airport is located at an altitude of 154 meters above sea level.

Missing data from the Landvetter Station was interpolated using linear interpolation. 42 values were missing from the temperature dataset, and 45 values were missing from the

relative humidity dataset. The missing values were primarily found in January, and therefore do not affect the analysis of this study, which is performed in July.

The dewpoint temperature was estimated with the following equation suggested by Lawrence (2005):

$$t_d = t - \left(\frac{100 - RH}{5}\right)$$

Equation 1. Dewpoint temperature.

Where t_d is the dewpoint temperature in degrees Celsius, t is the air temperature in degrees Celsius and RH is the relative humidity expressed as a percentage (Lawrence, 2005).

Data on air pressure, incoming short- and longwave radiation, diffuse shortwave radiation, wind direction, and wind speed were gathered from the rooftop station of the Department of Earth Sciences (GVC), at the University of Gothenburg. The station is located 72 meters above sea level. These 10-minute data were averaged for each hour, i.e., the values for 10.00 were averaged based on the 9.10-10.00 values.

The direct shortwave radiation was calculated according to an equation proposed by Lindberg et al. (2016):

$$K_{dir} = \frac{(K_{down} - K_{diff})}{\sin \eta}$$

Equation 2. Direct shortwave radiation.

Where K_{dir} is the direct shortwave radiation, K_{down} is the global solar radiation, K_{diff} is the diffuse solar radiation and η is the altitude of the sun expressed in radians (Lindberg et al., 2016). The altitudes were calculated using the SOLWEIG model (Lindberg et al., 2008), which is a model used for estimating radiation fluxes and mean radiant temperature. Since EQUATION 2 is sensitive to low numbers of the sun altitude (and generates unreasonably high numbers in these cases), all values of K_{dir} above 1400 were set to equal the values of K_{diff} instead.

Data on soil temperature (Muñoz Sabater, 2021) was downloaded from the Copernicus Climate Change Service (C3S) Climate Data Store. The soil temperature was downloaded for

three depths (0.035, 0.175, and 1.93 m) for June to October of 2021, and then averaged for each month. For the rest of the year default values were used.

3.2.3 Observed temperature data

To be able to evaluate how well the UWG model compares with actual temperature data, an observed dataset of air temperature is required. During the summer of 2021, the Göteborg Urban Climate Group at the University of Gothenburg collected temperature data on 20 different sites around Gothenburg (see FIGURE 3). Data were collected between June 28th and October 31st. Each sensor, of the type "Tinytag Plus 2" (sensor accuracy ±0.45°C) was placed at a height of around 2 meters and protected with a radiation shield. Air temperatures were measured every 10 minutes.

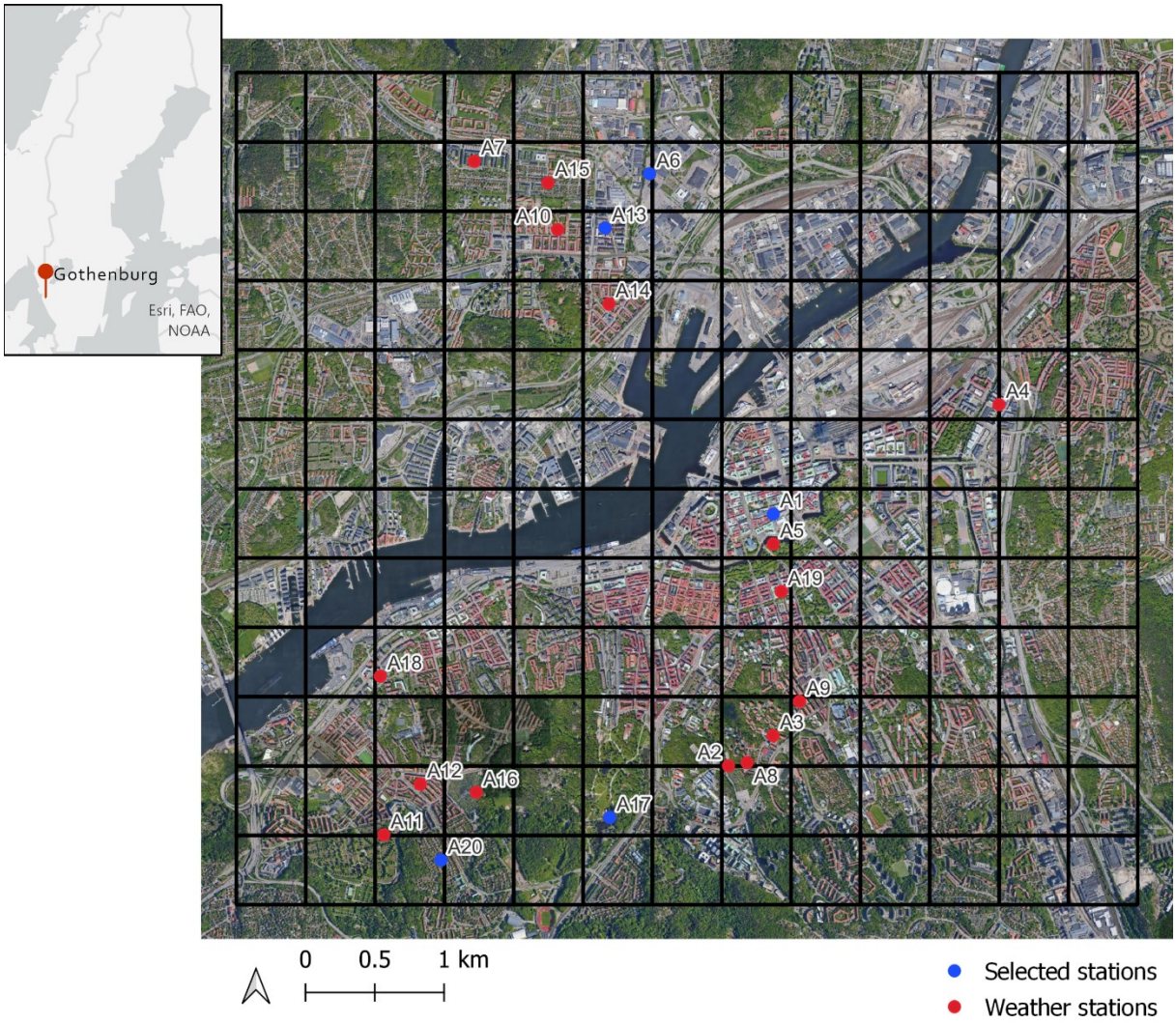

*Figure 3. Map of weather stations measuring air temperatures in Gothenburg in the summer of 2021. The blue points represent the stations selected for this study. The grid displays the larger area analyzed in this study, where more details are found in section **3.4**. Basemap: Esri Light Grey (overview map) & Google Satellite.*

3.3 Sensitivity analysis

To evaluate which parameters are mostly considered by the UWG, a sensitivity analysis was performed on a variety of parameters. The reason for performing this analysis includes the identification of what parameters are the most important to collect for users of the model (Nakano et al., 2015). Several parameters were selected for this study, and each was signed a standard value, as presented in TABLE 4. Thereafter three or four tests were performed for each of the parameters where the standard values were kept except for the parameter tested. All the tests were run for the month of July 2021. This resulted in new hourly air temperatures which were averaged for the whole month. The values of each test and the resulting modeled mean air temperature are presented in section **4.1**, TABLE 7. Since "Building Density", "Grass cover" and "Tree Cover" all are a fraction of the total area of the ground, the sum of these cannot be more than 1. Some of the parameters were also tested together, including Building Density + Vertical to Horizontal and Grass Cover + Tree Cover to see if the impact was larger than changing them by themselves. Also, a test was performed where the ground cover was set to only grass, trees, or paved. However, as the model is written now, it was not possible to set the three building parameters (Height, Density, Vertical to Horizontal) to zero. Therefore, the ground cover was set to 0.99 for each of these tests. All the building types were separately tested and set to 1 whereas the rest were set to 0 for each test.

Table 4. Parameters used in the sensitivity test and their standard values.

Parameters	**Standard**
Building Height [3] (m)	15
Building Density[4] (0-1)	0.3
Vertical to Horizontal[5] (ratio)	0.65
Grass Cover (0-1)	0.1
Tree Cover (0-1)	0.05
LatGrass [6] (0-1)	0.4
LatTree [7] (0-1)	0.6
Height UBL 1[8] (m)	1000
Height UBL 2[9] (m)	80

[3] Average building height (m)
[4] Horizontal building density
[5] Vertical to Horizontal ratio (façade area/urban area)
[6] Fraction of the heat absorbed by grass that is latent (goes to evaporating water)
[7] Fraction of the heat absorbed by trees that is latent (goes to evaporating water)
[8] Urban boundary layer height during day
[9] Urban boundary layer height during night

Building types (0-1)	
FullServiceRestaurant	0.4181
Hospital	0
LargeHotel	0
LargeOffice	0.0224
MedOffice	0
MidRiseApartment	0.5121
OutPatient	0
PrimarySchool	0
QuickServiceRestaurant	0
SecondarySchool	0.0243
SmallHotel	0
SmallOffice	0
StandAloneRetail	0
StripMall	0
SuperMarket	0
Warehouse	0.0231

3.4 Model evaluation

To evaluate how well the UWG predicts urban air temperatures, observed data are compared to modeled data. From the weather stations presented in section **3.2.3**, five of them were selected to use in the evaluation of the UWG. The selected stations represent different urban types with a variation in surrounding building attributes and fraction of vegetation, as presented in TABLE 5. A buffer zone with a 100-meter radius was created for each of the stations (the choice of this distance being suggested by for instance Eliasson & Svensson (2006)), presented in FIGURE 4. Then the UWG was run for each of these stations. As already described, the Landvetter station is located 154 meters above sea level. For this analysis, the Landvetter temperature was adjusted for height. Since the selected stations are located at various elevations the Landvetter temperature was adjusted down by 130 meters, i.e. 1.274 °C was added to the Landvetter air temperature data. This refers to the dry adiabatic lapse rate, which is the rate of cooling of a dry air parcel in a vertical direction, which is a reduction of 9.8 °C per kilometer of moving upwards in the atmosphere (Lutgens & Tarbuck, 2016). The relative humidity and dewpoint temperature were not changed.

The satellite images of each study area are presented in FIGURE 4 with a description of each area's urban setting in TABLE 5. The land cover and morphological parameters of each station are presented in TABLE 6. However, there was a slight discrepancy between the DSM and Land Cover raster layers for the Slottsskogen area, producing defective numbers. Therefore, the building density and Vertical-to-Horizontal values were manually set to 0.005.

Figure 4. The five selected areas of interest for this study. Basemap: Google Satellite.

Table 5. Description of weather stations selected for this study.

Station Number	Location	Urban setting
A1	Vallgatan	The city center of Gothenburg. Characterized by mid/high-rise dense buildings and a negligible fraction of vegetation.
A13	Kvillebäcken	Central Gothenburg. The eastern part of Kvillebäcken, also called "New Kvillebäcken". Characterized by relatively newly built dense high-rise apartment buildings and a low fraction of vegetation.
A6	Backaplan	Central Gothenburg. Area mostly consisting of parking lots and warehouses or department stores. Low fraction of vegetation.
A20	Kungsladugård	House in Kungsladugård, located about 3 km from the city center. Area characterized by residential low-rise houses. Gardens with grass lawns and trees.
A17	Slottsskogen	Central Gothenburg. Urban park, vegetation type varies between grass lawns and mostly deciduous trees. The weather station is located near the pond in the park.

Table 6. UWG input values of the main parameters of the 5 selected stations, calculated by "UWG Prepare" in UMEP.

	Vallgatan	Kvillebäcken	Backaplan	Kungsladugård	Slottsskogen
Building Height	14.61	18.461	6.909	6.942	6.744
Building Density	0.658	0.399	0.381	0.205	0.005
Vertical to Horizontal	0.776	1.234	0.199	0.374	0.005
Grass Cover	0.013	0.083	0.048	0.155	0.223
Tree Cover	0.021	0.087	0.033	0.302	0.465

The output was then analyzed for a shorter period of time (see results in section **4.2.1**). This period was chosen as July 20th-28th, which had relatively high air temperatures, and a mixture of weather conditions. Air temperatures of Landvetter, wind direction, wind speed, and radiation of this period, are presented in FIGURE 5. The conditions for the formation of a UHI are most ideal on the first nights, from the 20th to the 25th, where there was low wind speed during the night and no cloudiness either day or night (except on the night of the 23rd – 24th). The later part of this time period has more clouds and is windier during the night.

A statistical analysis for the whole month of July was also performed (results in section **4.2.2**). The difference in air temperatures (i.e. the UHI intensity) between the rural reference and the observed/modeled data was averaged for each night, when incoming shortwave radiation was <5 w/m^2. The results are then presented as boxplots where the average UHI intensities of the observed data and the modeled data are compared to each other. The

maximum UHI intensity for each night was also analyzed but showed similar patterns to the average UHI intensities and is therefore presented in **Appendix A**.

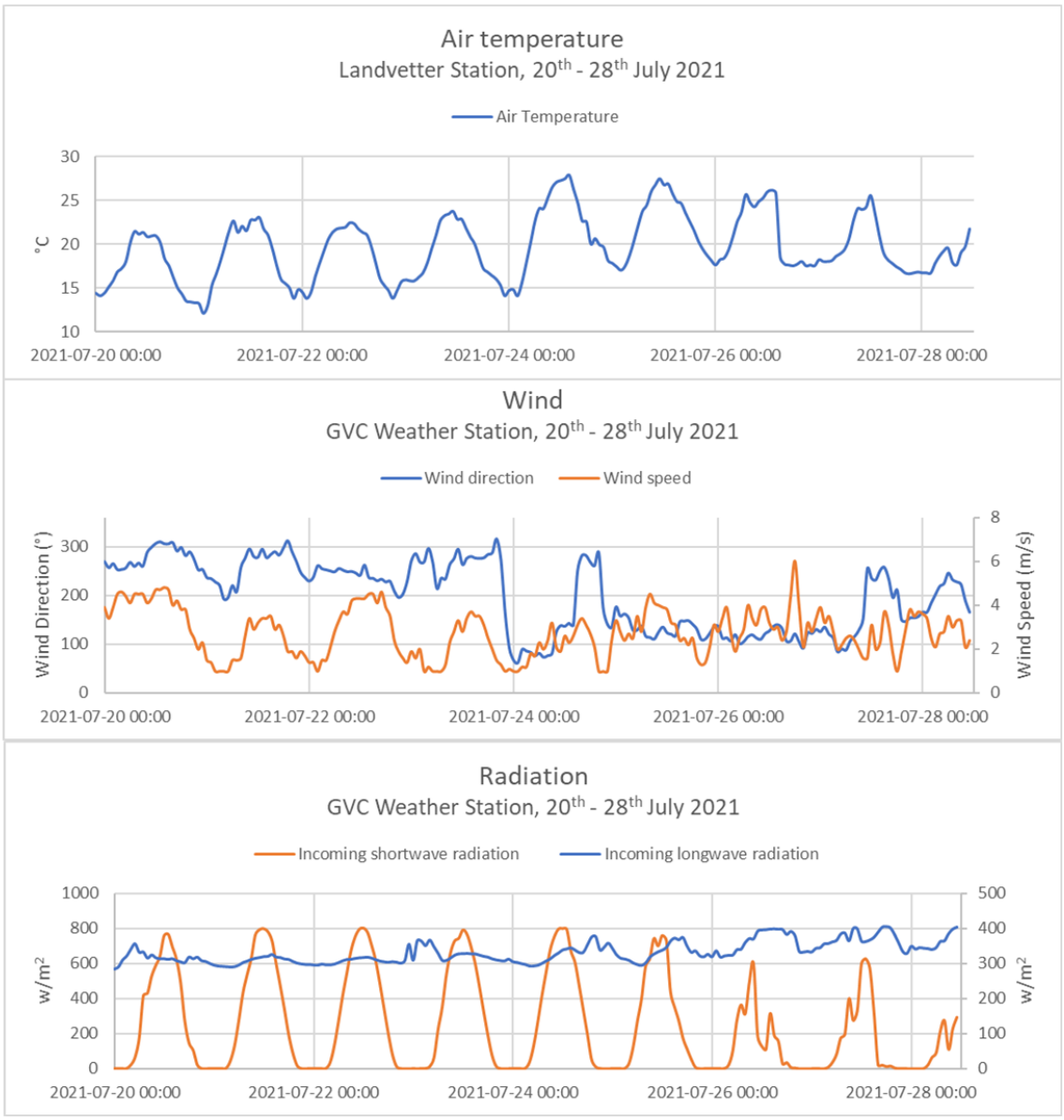

Figure 5. Air temperatures, wind conditions, and incoming short- and longwave radiation for the analyzed period of July 20th-28th 2021.

Finally, a 500-m grid was constructed for a larger part of central Gothenburg, and the model was run for July for this larger grid as well (results in **4.2.3**). The purpose of this analysis is to see how the model performs on a larger scale, and if this result can be connected to the result of previously mentioned analyses.

4 Results

4.1 Sensitivity analysis

The result of the sensitivity analysis is presented as the modeled mean air temperature for July 2021 in TABLE 7. A standard test with the values of TABLE 4 was performed where the resulting modeled mean air temperature was 19.59 °C.

Table 7. Results of the sensitivity analysis, expressed as the modeled average air temperatures for July

	Test 1	Test 2	Test 3	Test 4
Building Height (m)	5	10	20	25
Modeled mean air temperature July (°C)	19.48	19.53	19.66	19.74
Building Density (0-1)	0.1	0.5	0.7	0.85
Modeled mean air temperature July (°C)	19.45	19.81	20.19	21.05
Vertical to Horizontal (ratio)	0.3	0.9	1.2	1.4
Modeled mean air temperature July (°C)	19.58	19.60	19.61	19.62
Grass Cover (0-1)	0.05	0.2	0.4	0.6
Modeled mean air temperature July (°C)	19.59	19.58	19.58	19.57
Tree Cover (0-1)	0	0.1	0.3	0.6
Modeled mean air temperature July (°C)	19.59	19.59	19.59	19.59
LatGrass (0-1)	0.2	0.6	0.8	1
Modeled mean air temperature July (°C)	19.57	19.61	19.64	-
LatTree (0-1)	0.2	0.4	0.8	1
Modeled mean air temperature July (°C)	19.59	19.59	19.59	-
Height UBL 1 (m)	900	950	1050	1100
Modeled mean air temperature July (°C)	19.59	19.59	19.59	19.59
Height UBL 2 (m)	60	70	90	100
Modeled mean air temperature July (°C)	19.52	19.55	19.59	19.62
Building Density + Vertical to Horizontal				
Building Density (0-1)	0.1	0.5	0.7	0.85
Vertical to Horizontal (ratio)	0.3	0.9	1.2	1.4
	19.45	19.82	20.20	21.07
Grass Cover + Tree Cover				
Grass Cover (0-1)	0.05	0.2	0.4	
Tree Cover (0-1)	0	0.1	0.3	
Modeled mean air temperature July (°C)	19.59	19.58	19.57	
Vegetation/paved				
Paved (0-1)	0.99	0	0	
Grass Cover (0-1)	0	0.99	0	
Tree Cover (0-1)	0	0	0.99	
Modeled mean air temperature July (°C)	19.41	19.34	19.40	
Building types (0-1)				
FullServiceRestaurant	1			
Modeled mean air temperature July (°C)	19.79			
Hospital	1			
Modeled mean air temperature July (°C)	19.53			
LargeHotel	1			
Modeled mean air temperature July (°C)	19.54			

LargeOffice	1			
Modeled mean air temperature July (°C)	19.48			
MedOffice	1			
Modeled mean air temperature July (°C)	19.49			
MidRiseApartment	1			
Modeled mean air temperature July (°C)	19.45			
OutPatient	1			
Modeled mean air temperature July (°C)	19.53			
PrimarySchool	1			
Modeled mean air temperature July (°C)	19.49			
QuickServiceRestaurant	1			
Modeled mean air temperature July (°C)	19.81			
SecondarySchool	1			
Modeled mean air temperature July (°C)	19.48			
SmallHotel	1			
Modeled mean air temperature July (°C)	19.50			
SmallOffice	1			
Modeled mean air temperature July (°C)	19.48			
StandAloneRetail	1			
Modeled mean air temperature July (°C)	19.46			
StripMall	1			
Modeled mean air temperature July (°C)	19.48			
SuperMarket	1			
Modeled mean air temperature July (°C)	19.46			
Warehouse	1			
Modeled mean air temperature July (°C)	19.42			

The result of the sensitivity test for Building Height shows that changing the parameter did not affect the result namely compared to the standard test. The mean of all tests is within a range of 0.15 °C compared to the standard value. The Building Density test had the most substantial effect compared to the standard value of all the sensitivity tests. The greatest difference is seen in Test 4, which has an almost 1.5 °C higher mean than the standard test. The sensitivity test for the Vertical to Horizontal parameter shows no notable difference from the standard values. The range of the mean for all tests is within 0.03 °C from the mean of the standard values. When changing the Building Density and Vertical to Horizontal parameters simultaneously, this did affect the modeled air temperatures compared to the standard test. However, compared to the results when changing only Building Density, there is not a much larger effect.

The sensitivity test of changing the Tree Cover and Grass Cover did not have any substantial effects on the modeled air temperature. The mean is not changed at all for the Tree Cover tests, while the mean of the Grass Covered altered marginally in three of the tests, with the

highest decrease for Test 4, of 0.02 °C. Also, changing these parameters synchronously did not have a large effect on the air temperatures either.

The sensitivity test for when the ground is 99 % covered by grass, paved, and trees, respectively, results in a marginally lower mean for all three tests compared to the standard values. The lowest mean has the grass cover, 0.25 °C lower than the standard mean.

Changing the different Building types resulted in a maximum difference of 0.22 °C higher mean (for "QuickServiceRestaurant") than the standard test. The "Warehouse" lowered the mean air temperatures the most, by 0.17 °C.

4.2 Model evaluation

The results of the model evaluation are presented in sections **4.2.1, 4.2.2,** and **4.2.3**.

4.2.1 Temporal analysis of selected areas for 20th-28th of July

An hourly comparison of observed and UWG data is presented in this section. The air temperatures of the rural reference (Landvetter) are also displayed to identify the UHI off each night.

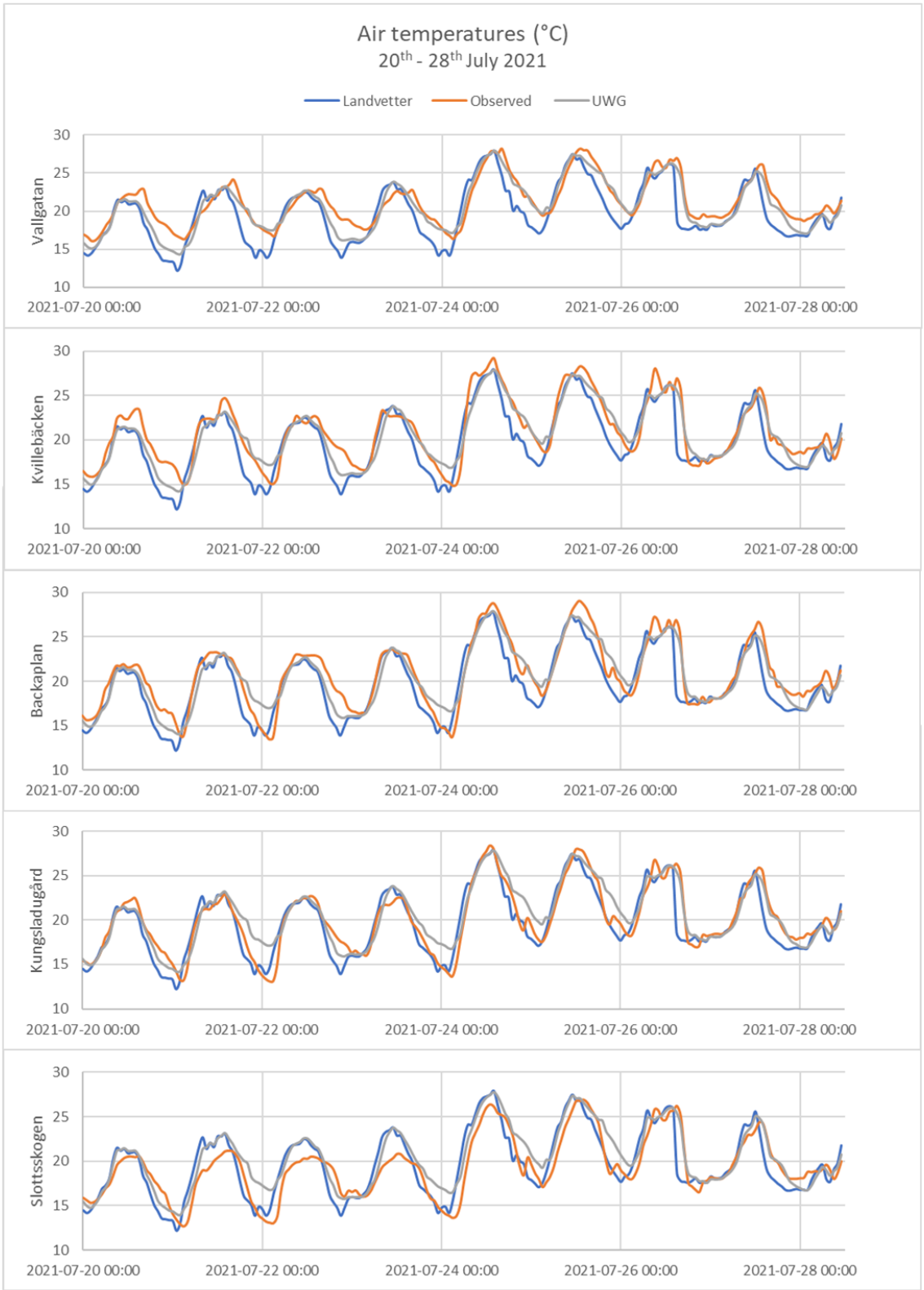

Figure 6. Hourly values of rural, observed, and modeled data at the five selected stations, July 20th-28th 2021.

At Vallgatan, the rural and urban observational data show that a UHI can be identified for all nights of the period. However, the modeled data underestimates the UHI effect on the nights of the 20th-21st, 22nd-23rd, 26th-27th, and 27th-28th of July. The maximum difference between modeled and observed data occurred on the night of July 22nd-23rd with a temperature difference of 2.75 °C.

In Kvillebäcken, a UHI can be identified for all nights except on the 26th-27th. The model underestimates the UHI on the 20th-21st, 22nd-23rd, and 27th-28th, while it instead overestimates the UHI on the nights of 21st-22nd and 23rd-24th. On the 22nd-23rd the largest difference between UWG and observed data occurred, with an underestimation from the model of 3.03 °C.

The modeled data of Backaplan show similar patterns as in Kvillebäcken, with under- and overestimations occurring on the same nights. Also, there is no observed UHI on the night of the 26th-27th. The largest maximum difference between observed and modeled is found on the 21st-22nd, where the modeled data was 3.55 °C higher than the observed.

For Kungsladugård, there is a UHI observed on the nights of July 20th-21st, 22nd-23rd, and 27th-28th. On the nights of the 21st-22nd, and 23rd-26th the UWG overestimates the UHI effect. The maximum difference between UWG and observed data, 4.02 °C, is found on the nights of 21st-22nd.

The effect vegetation has on air temperatures is clearest observed in Slottsskogen (but also Kungsladugård), where the observed data sometimes is lower than the rural reference. There is a small UHI effect on the 21st, 23rd, and 28th of July. Like Kungsladugård, the UWG overestimates the air temperatures on the 21st-22nd, and 23rd-26th, while it slightly underestimates the temperatures on the 27th-28th. The maximum difference between modeled and observed data occurred on the 22nd with a temperature difference of 3.8 °C.

4.2.2 Statistical analysis of selected stations

The average UHI Intensity for July is presented in this section.

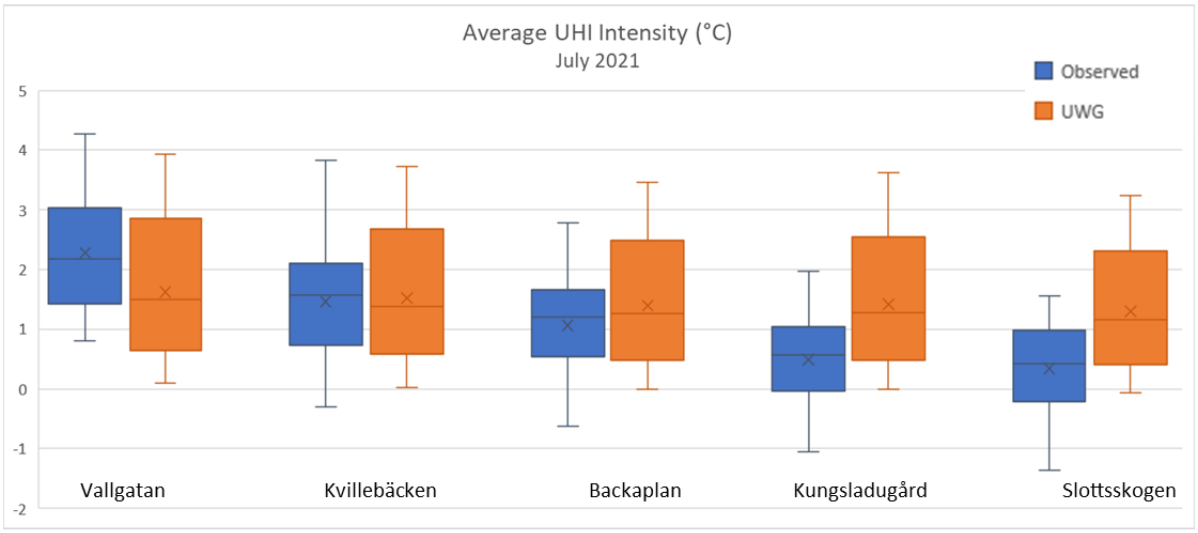

Figure 7. Boxplots of the average UHI intensity at night, of observed and modeled data at each of the study sites.

The analysis of the whole of July shows that the modeled data somewhat underestimates the UHI intensity of Vallgatan. Both the median and mean for the modeled data are lower than the observed data at this site, where the mean is 0.7 °C lower.

For Kvillebäcken, the UWG average UHI intensity is quite consistent with the observed data. The mean of the observed data is 1.46 °C while the mean of the observed data is 1.52 °C.

For Backaplan the result indicates that the UWG makes a small overestimation of the UHI, although the medians of the two boxes are quite close to each other. However, the mean value is slightly higher for the modeled data, at about 0.3 °C.

For Kungsladugård the modeled data is overestimating the air temperatures. The mean is almost 1 °C lower than the observed data. The highest UHI intensity of the observed data is 1.97 °C while the highest value for the UWG is 3.6 °C.

With a mean of 0.34, Slottsskogen has the lowest observed mean of the five selected stations, as well as the lowest maximum and minimum temperatures. This means that the UHI is least prevalent in this station out of the selected ones. The mean for the UWG is 1.30 °C, so the UWG overestimates the air temperatures compared to the observed data. The

highest value of the observed data is 1.56 °C, while the highest value of the modeled data is 3.2 °C.

4.2.3 Modeling the UHI on a city-scale

In this section, the results of the UWG simulations for a larger part of Gothenburg are presented (FIGURE 8), on the night of July 24th-25th.

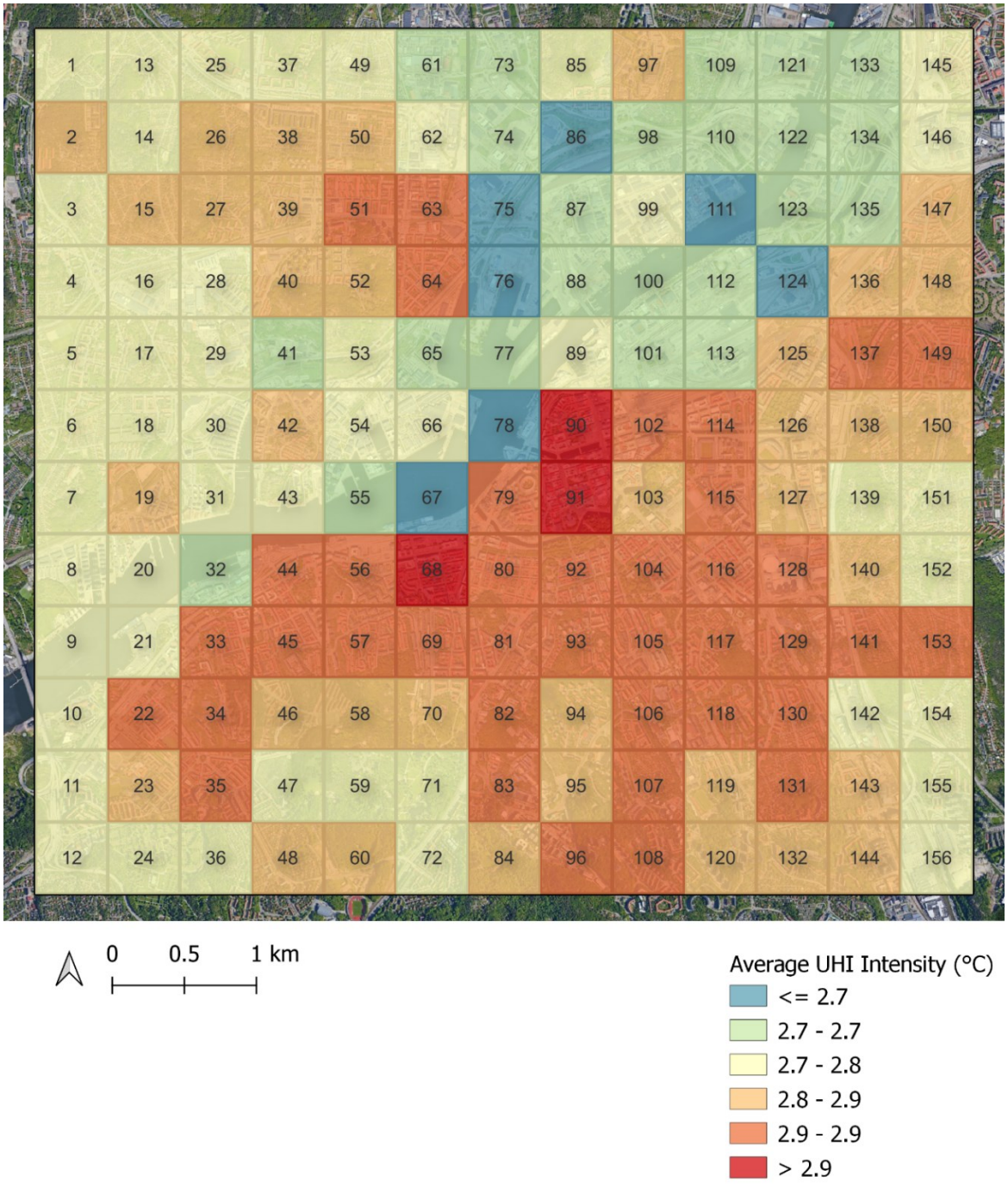

Figure 8. The average UHI on the night of July 24th-25th. Basemap: Google Satellite.

The largest modeled UHI:s are seen in grid 68, 90 and 91 which are all built-up dense areas in the city center. The lowest UHI:s, are found in areas with water and in open areas. These open areas (grid 75, 76, 86, 124) are both grass-covered and paved, and lack high and dense buildings. Larger parks such as Slottsskogen (which is found in approximately grid 47, 58, 59, 60, 70, and 71) have a medium average UHI intensity using this scale.

5 Discussion

This section discusses the results of the sensitivity analysis and the model evaluation. It also discusses the limitations of this study and some suggestions for future research.

5.1 Sensitivity analysis

In the first published paper of UWG, Bueno et al. (2013) performed a sensitivity analysis where the Building Density, Vertical to Horizontal, and to some extent Vegetation parameters were the most influential. What the sensitivity analysis of this case study demonstrates is that the UWG is not very sensitive to the different parameters except for the Building Density TABLE 7. The different building types did not have a remarkable impact on the estimated air temperatures, where "QuickServiceRestaurant" and "FullServiceRestaurant" had the largest difference when compared to the standard test. Noticeable was also that vegetation was not significantly considered by the model. This is in accordance with the results from the model evaluation, where it seemed like temperatures at sites with a high fraction of vegetation generally were overestimated by the model. As presented in section **2.2.3**, many studies have confirmed the mitigation effect vegetation has on air temperatures in an urban area. Therefore, the results of the sensitivity analysis were quite surprising. When changing the ground cover parameters to 99% there was a slight change where the grass cover lowered the temperatures the most. If only looking at night-time temperatures this would not have been surprising, since tree canopies can trap some heat and radiation (Konarska et al., 2016). Though, this sensitivity analysis was performed on 24-hour data, which would suggest a lowering of air temperatures where a lot of trees are present since they provide shade and evaporation during daytime (Spronken-Smith & Oke, 1999). Summarizing the sensitivity analysis, it was foreseen that changing the building parameters would influence the results, but more surprising that the vegetation has such a small (or absent) effect, and that this also affects the performance results of the model. Also,

the different building types were not very sensitive when changed, which reduces the need for very detailed data.

5.2 Model evaluation

Generally, there seems to be a better agreement between observed and modeled data on the urban, built-up areas such as Vallgatan, Kvillebäcken, and Backaplan for the study period of 20th– 28th of July, in accordance with the results of Salvati et al. (2016), where also the urban built-up areas had the highest agreement with the UWG. Both Kungsladugård and Slottsskogen are mostly overestimated by the model. Looking at the box plots in FIGURE 7, where the UHI intensity was analyzed for July, they suggest the same patterns. Vallgatan is slightly underestimated, Kvillebäcken and Backaplan are quite consistent with the observed data, while Kungsladugård and Slottsskogen are overestimated. This section will present a discussion on possible explanations of these results.

5.2.1 Urban geometry and vegetation

Vallgatan, Kvillebäcken, and Backaplan are characterized by their urban features with a low fraction of vegetation. The air temperatures of Vallgatan are slightly underestimated by the model, but in general, the model follows the pattern of the UHI:s at these stations, at least looking at the whole month of July (FIGURE 7). For Kungsladugård, where there is a built-up area, but the fraction of vegetation is higher, and Slottsskogen has the highest amount of vegetation of all the areas of this study. It is quite clear that the model is not handling the presence of vegetation when calculating the urban temperatures, since both Kungsladugård and Slottsskogen are overestimated both on the period of 20th - 28th of July and for the whole month of July (FIGURE 6 and FIGURE 7). At least half of the days are overestimated, and the days that are not, are instead underestimated in the rest of the areas. As both Kungsladugård and Slottsskogen are characterized by a large fraction of vegetation, and the sensitivity analysis showed that the modeled data lacked consideration of vegetation, it can be assumed that it is the vegetation that affects the results of these areas. This is also in line with the results of Salvati et al. (2016), where the UWG was evaluated for Rome and Barcelona. The conclusion there was that the model did not consider the influence of vegetation sufficiently, which can be concluded in this study as well. Backaplan had both under- and overestimations looking only at July 20th-28th. This is a quite open area with lots of impervious surfaces, so instead of vegetation, there might be other factors influencing the

results of the model, such as wind speed or wind direction, the heat storage or the albedo of the buildings. Or, just that the area is more open and therefore the radiative cooling is faster than for the more built-up areas, and in that case, the model does not capture this sufficiently.

5.2.2 Meteorological parameters

5.2.2.1 Cloud cover

Another factor that could explain the differences between modeled and observed data are the meteorological parameters and the fact that they are gathered from different weather stations. For instance, there is increased long-wave radiation on the nights of July 22nd-23rd, and 25th-28th, which indicates the presence of clouds on these nights. On the night of July 22nd-23rd, the model is underestimating the air temperatures on all five study sites, and the model tends to underestimate air temperatures also on the nights of July 26th-27th and 27th-28th at some sites. This would agree with the theoretical background, saying that the presence of clouds lowers the development of the UHI. However, the model is underestimating the air temperatures also on the 21st-22nd, where there is no cloudiness observed. Moreover, looking at the night of the 22nd-23rd, it is cloudy in Gothenburg (FIGURE 5), which would suggest a lower UHI intensity, as considered in section **2.2.5**, but there is a quite large observed UHI between the urban sites and the Landvetter data. If only looking at this parameter, the UHI effect actually seen implies that there were no clouds on the rural site. However, since input data come from both Gothenburg (the radiation data) and Landvetter (air temperature data), this might have affected the results. Furthermore, since the type and thickness of cloud cover (Morris et al., 2001) also affect the magnitude of the UHI this might be another explanation, which has not been analyzed in the scope of this study. In summary, the presence or non-presence of clouds by itself is not enough to explain the variations of the model output.

5.2.2.2 Wind parameters

Considering the wind parameters, winds are more or less westerly on the 20th- 24th, which one could assume would bring cool air from the ocean. It is also assumed that Backaplan, Kungsladugård, and Slottsskogen would be most affected by winds. In Vallgatan and Kvillebäcken, the winds are most likely blocked by the tall and dense buildings (Salvati et al., 2017; van Hove et al., 2015). The model is overestimating the air temperatures on the 21st-

22nd and 23rd-24th but not on the 20th-21st or 22nd-23rd in Backaplan, Kungsladugård, and Slottsskogen. Consequently, there is no clear pattern of how westerly winds affect the results. Results from the study by Salvati et al. (2016) suggest that the UWG does not consider the cooling effect of the sea breeze, a phenomenon that has not been examined in this study. However, just assuming that westerly winds in Gothenburg bring cooler air into the city, the short-time period examined in this case study does not bring any consensus on whether this is the case in Gothenburg.

The days examined in this study were chosen as optimal days for UHI formation, therefore the wind speed of the nights is low (average wind speed of the five first nights is < 2 m/s while it is between 2.38-3.25 m/s on the last four nights) and cannot be assigned a large influence of the results. A final note is also that the wind direction and wind speeds might be different at the study sites than at the GVC station with a higher elevation. For more exact results, wind direction and wind speed should have been measured at each study site.

5.2.3 Scale

Looking at the analysis for the larger part of Gothenburg (FIGURE 8), the results are mostly as expected, where the most urban and dense areas have the highest UHI intensities, and the water, and the open areas are the coolest. The vegetated areas are modeled a low-medium UHI intensity in general. From what is known from the first part of the model evaluation, one could argue that the built-up areas should be even warmer (considering the results of Vallgatan), while the vegetated areas should be even cooler. Considering only the grids with the lowest UHI intensities, it seems like it is the absence of buildings rather than the influence of vegetation that creates the smallest UHI:s by the model.

What is important to consider is that this model is mainly developed as a local scale model and that it has limitations in regards to capturing micro-scale properties (Bueno et al., 2014). Therefore, one should not expect a complete model from a micro-scale point of view, but a more general estimation of the air temperatures. This approach is mainly applicable to the built-up urban areas, whereas the model needs improvement in capturing the cooling effect of vegetation.

5.3 Method and data limitations

There are some potential sources of errors that need to be taken into consideration when reflecting on this study and evaluating the model. For instance, the rural station is on a higher elevation, and although this was considered when running the model, the interconnected parameters of relative humidity and dewpoint were not adjusted for height. Also, the difference in location between Landvetter station (temperature and relative humidity) and the GVC station (i.e. the data of wind and radiation) could have affected the outcome. Differences in weather can be found along quite short distances, so for instance some cloudy days/hours in Gothenburg, are not necessarily seen in Landvetter at the same time. Also, since Landvetter is located more inland than Gothenburg, there are limitations when comparing it to observed data in Gothenburg, which should be more influenced by the ocean.

Another limiting factor is that the rural station is placed on the airport of Landvetter. This could mean that there is an urban influence on the air temperatures also on this site, as found for instance in the airport of Rotterdam (van Hove et al., 2015). Other available options for use as a rural reference (such as observed temperatures of Åbyvallen or Slottsskogen) were also investigated, but the temperatures of Landvetter were estimated to have the least urban influence of these alternatives.

Finally, there are some possible errors from the observed (Gothenburg) data as well. The sensors have an accuracy of ±0.45°C, which could have affected the outcome when compared to modeled data. Also, the location of the sensors could be impacted by very local microclimate and therefore have an impact on the results. For instance, the sensor at Vallgatan is located close to a wall, which could explain why the observed data there is higher than the modeled data. At Backaplan, the sensor is quite close to trees and the small river, which might also influence the observed air temperatures.

5.4 Future research

For future research, there is a need to further investigate how the UWG can be improved to predict air temperatures with the presence of vegetation. A new urban climate model called “the Vertical City Weather Generator (VCWG)” (Moradi et al., 2021) which combines components of the UWG with other climate models could also be analyzed and evaluated to

see if urban air temperatures are modeled more correctly. For instance, this model considers the influence of trees and vegetation to a greater extent (Moradi et al., 2021).

Other parameters, such as the albedo of the buildings, relative humidity, and the thermal properties of specific materials, which have not been explored in the scope of this study, could also be of interest for further investigations.

6 Conclusion

In conclusion, this study has examined and evaluated the Urban Weather Generator, in terms of how well it predicts Urban Heat Islands in Gothenburg. A sensitivity analysis and a model evaluation have been carried out. The results of the sensitivity analysis indicate that the emphasis of the model is the building parameters, whereas vegetation is less considered by the model. The results of the sensitivity analysis are also reflected in the model evaluation, where vegetated areas are overpredicted by the model, whereas built-up areas are predicted more correctly. No clear relationship between the days when the model estimates inadequately and other parameters are seen. There is an indication that cloudy nights are more underpredicted by the model than cloud-free. Neither the wind direction nor wind speed can be assigned any significant influence on the results of this study, but in order to see these patterns, the data should have been analyzed for a longer period of time. Difficulties in finding these explanations could also be referred to the fact that the rural and urban areas are located at different distances from the ocean, as well as at different elevations above sea level. The results of this study could also conclude that the UWG performs better on rather urbanized areas, hence the performance of the model would be optimized in cities with a minor fraction of vegetation.

7 Appendix A

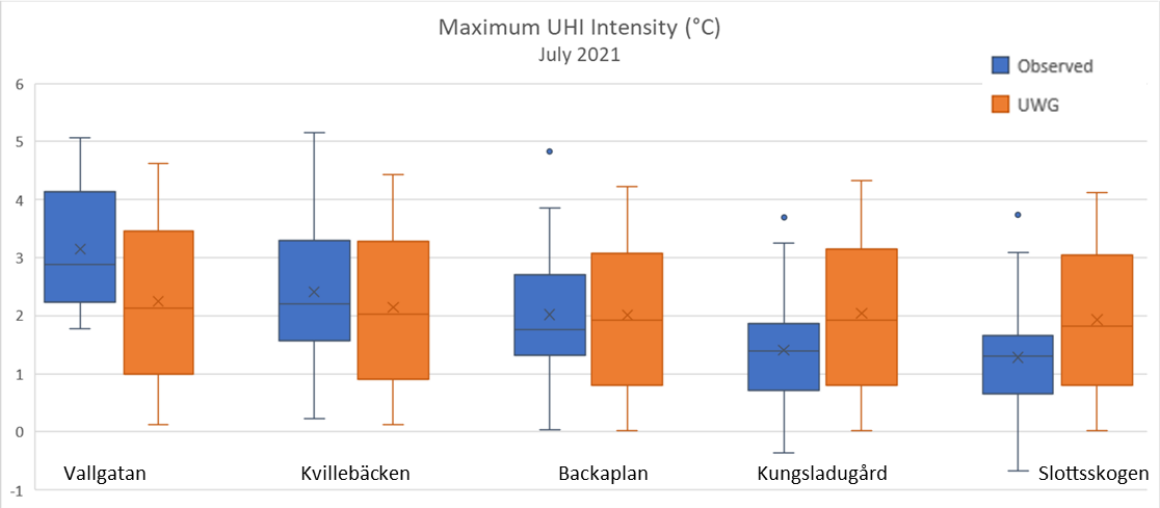

8 References

Bueno, B., Norford, L., Hidalgo, J., & Pigeon, G. (2013). The urban weather generator. Journal of Building Performance Simulation, 6(4), 269–281. https://doi.org/10.1080/19401493.2012.718797

Bueno, B., Pigeon, G., Norford, L. K., Zibouche, K., & Marchadier, C. (2012). Development and evaluation of a building energy model integrated in the TEB scheme. Geoscientific Model Development, 5(2), 433–448. https://doi.org/10.5194/gmd-5-433-2012

Bueno, B., Roth, M., Norford, L., & Li, R. (2014). Computationally efficient prediction of canopy level urban air temperature at the neighbourhood scale. Urban Climate, 9, 35–53. https://doi.org/10.1016/j.uclim.2014.05.005

Chow, W. T. L., & Roth, M. (2006). Temporal dynamics of the urban heat island of Singapore. International Journal of Climatology, 26(15), 2243–2260. https://doi.org/10.1002/joc.1364

Coutts, A. M., Beringer, J., & Tapper, N. J. (2007). Impact of Increasing Urban Density on Local Climate: Spatial and Temporal Variations in the Surface Energy Balance in Melbourne, Australia. Journal of Applied Meteorology and Climatology, 46(4), 477–493. https://doi.org/10.1175/JAM2462.1

Eliasson, I., & Svensson, M. (2006). Spatial air temperature variations and urban land use—A statistical approach. Meteorological Applications, 10, 135–149. https://doi.org/10.1017/S1350482703002056

Erell, E., Pearlmutter, D., Boneh, D., & Kutiel, P. B. (2014). Effect of high-albedo materials on pedestrian heat stress in urban street canyons. Urban Climate, 10, 367–386. https://doi.org/10.1016/j.uclim.2013.10.005

Erell, E., & Williamson, T. (2007). Intra-urban differences in canopy layer air temperature at a mid-latitude city. International Journal of Climatology, 27(9), 1243–1255. https://doi.org/10.1002/joc.1469

Fischer, E. M., Oleson, K. W., & Lawrence, D. M. (2012). Contrasting urban and rural heat stress responses to climate change. Geophysical Research Letters, 39(3). https://doi.org/10.1029/2011GL050576

Grimmond, S. (2007). Urbanization and global environmental change: Local effects of urban warming. The Geographical Journal, 173(1), 83–88. https://doi.org/10.1111/j.1475-4959.2007.232_3.x

Haeger-Eugensson, M., & Holmer, B. (1999). Advection caused by the urban heat island circulation as a regulating factor on the nocturnal urban heat island. International Journal of Climatology, 19(9), 975–988. https://doi.org/10.1002/(SICI)1097-0088(199907)19:9<975::AID-JOC399>3.0.CO;2-J

Hardin, A. W., Liu, Y., Cao, G., & Vanos, J. K. (2018). Urban heat island intensity and spatial variability by synoptic weather type in the northeast U.S. Urban Climate, 24, 747–762. https://doi.org/10.1016/j.uclim.2017.09.001

Holmer, B., Thorsson, S., & Eliasson, I. (2007). Cooling Rates, Sky View Factors and the Development of Intra-Urban Air Temperature Differences. Geografiska Annaler. Series A, Physical Geography, 89(4), 237–248.

Howard, L. (1833). The Climate of London deduced from meteorological observations. Harvey and Darton.

IPCC. (2021). Climate Change 2021: The Physical Science Basis. Contribution of Working Group I to the Sixth Assessment Report of the Intergovernmental Panel on Climate Change [Masson-Delmotte, V., P. Zhai, A. Pirani, S.L. Connors, C. Péan, S. Berger, N. Caud, Y. Chen, L. Goldfarb, M.I. Gomis, M. Huang, K. Leitzell, E. Lonnoy, J.B.R. Matthews, T.K. Maycock, T. Waterfield, O. Yelekçi, R. Yu, and B. Zhou (eds.)]. Cambridge University Press, Cambridge, United Kingdom and New York, NY, USA, In press, doi:10.1017/9781009157896

Johansson, S. (2018). The Influence of Land Cover on the Urban Energy Balance of Gothenburg. 52.

Konarska, J., Holmer, B., Lindberg, F., & Thorsson, S. (2016). Influence of vegetation and building geometry on the spatial variations of air temperature and cooling rates in a high-latitude city. International Journal of Climatology, 36(5), 2379–2395. https://doi.org/10.1002/joc.4502

Kuttler, W. (2008). The Urban Climate – Basic and Applied Aspects. In J. M. Marzluff, E. Shulenberger, W. Endlicher, M. Alberti, G. Bradley, C. Ryan, U. Simon, & C. ZumBrunnen (Eds.), Urban Ecology: An International Perspective on the Interaction

Between Humans and Nature (pp. 233–248). Springer US. https://doi.org/10.1007/978-0-387-73412-5_13

Lawrence, M. G. (2005). The Relationship between Relative Humidity and the Dewpoint Temperature in Moist Air: A Simple Conversion and Applications. Bulletin of the American Meteorological Society, 86(2), 225–234. https://doi.org/10.1175/BAMS-86-2-225

Lindberg, F. (2007). Modelling the urban climate using a local governmental geo-database. Meteorological Applications, 14(3), 263–273. https://doi.org/10.1002/met.29

Lindberg, F., Grimmond, C. S. B., Gabey, A., Huang, B., Kent, C. W., Sun, T., Theeuwes, N. E., Järvi, L., Ward, H. C., Capel-Timms, I., Chang, Y., Jonsson, P., Krave, N., Liu, D., Meyer, D., Olofson, K. F. G., Tan, J., Wästberg, D., Xue, L., & Zhang, Z. (2018). Urban Multi-scale Environmental Predictor (UMEP): An integrated tool for city-based climate services. Environmental Modelling & Software, 99, 70–87. https://doi.org/10.1016/j.envsoft.2017.09.020

Lindberg, F., Holmer, B., & Thorsson, S. (2008). SOLWEIG 1.0 – Modelling spatial variations of 3D radiant fluxes and mean radiant temperature in complex urban settings. International Journal of Biometeorology, 52(7), 697–713. https://doi.org/10.1007/s00484-008-0162-7

Lindberg, F., Onomura, S., & Grimmond, C. S. B. (2016). Influence of ground surface characteristics on the mean radiant temperature in urban areas. International Journal of Biometeorology, 60(9), 1439–1452. https://doi.org/10.1007/s00484-016-1135-x

Lutgens, F. K., & Tarbuck, E. J. (2016). The atmosphere: An introduction to meteorology (13e ed.). Pearson.

Mirzaei, P. A., Haghighat, F., Nakhaie, A. A., Yagouti, A., Giguère, M., Keusseyan, R., & Coman, A. (2012). Indoor thermal condition in urban heat Island – Development of a predictive tool. Building and Environment, 57, 7–17. https://doi.org/10.1016/j.buildenv.2012.03.018

Moradi, M., Dyer, B., Nazem, A., Nambiar, M. K., Nahian, M. R., Bueno, B., Mackey, C., Vasanthakumar, S., Nazarian, N., Krayenhoff, E. S., Norford, L. K., & Aliabadi, A. A. (2021). The Vertical City Weather Generator (VCWG v1.3.2). Geoscientific Model Development, 14(2), 961–984. https://doi.org/10.5194/gmd-14-961-2021

Morris, C. J. G., Simmonds, I., & Plummer, N. (2001). Quantification of the Influences of Wind and Cloud on the Nocturnal Urban Heat Island of a Large City. Journal of Applied Meteorology and Climatology, 40(2), 169–182. https://doi.org/10.1175/1520-0450(2001)040<0169:QOTIOW>2.0.CO;2

Muñoz Sabater, J. (2021). ERA5-Land hourly data from 1950 to 1980. Copernicus Climate Change Service (C3S) Climate Data Store (CDS).

Nakano, A., Bueno, B., Norford, L., & Reinhart, C. F. (2015). Urban Weather Generator—A Novel Workflow for Integrating Urban Heat Island Effect within Urban Design Process. MIT Web Domain. https://dspace.mit.edu/handle/1721.1/108779

Oke, T. R. (1982). The energetic basis of the urban heat island. Quarterly Journal of the Royal Meteorological Society, 108(455), 1–24. https://doi.org/10.1002/qj.49710845502

Oke, T. R., Mills, G., Christen, A., & Voogt, J. A. (2017). Urban Climates. Cambridge University Press. https://doi.org/10.1017/9781139016476

Onomura, S., Holmer, B., Lindberg, F., & Thorsson, S. (2016). Intra-urban nocturnal cooling rates: Development and evaluation of the NOCRA model. Meteorological Applications, 23(3), 339–352. https://doi.org/10.1002/met.1558

Park, H.-S. (1986). Features of the heat island in seoul and its surrounding cities. Atmospheric Environment (1967), 20(10), 1859–1866. https://doi.org/10.1016/0004-6981(86)90326-4

Ramírez-Aguilar, E. A., & Lucas Souza, L. C. (2019). Urban form and population density: Influences on Urban Heat Island intensities in Bogotá, Colombia. Urban Climate, 29, 100497. https://doi.org/10.1016/j.uclim.2019.100497

Sailor, D. J., & Lu, L. (2004). A top–down methodology for developing diurnal and seasonal anthropogenic heating profiles for urban areas. Atmospheric Environment, 38(17), 2737–2748. https://doi.org/10.1016/j.atmosenv.2004.01.034

Salvati, A., Coch Roura, H., & Cecere, C. (2016). Urban heat island prediction in the mediterranean context: An evaluation of the urban weather generator model. ACE: Architecture, City and Environment, 11(32), 135–156. https://doi.org/10.5821/ace.11.32.4836

Salvati, A., Coch Roura, H., & Cecere, C. (2017). Assessing the urban heat island and its energy impact on residential buildings in Mediterranean climate: Barcelona case study. Energy and Buildings, 146, 38–54. https://doi.org/10.1016/j.enbuild.2017.04.025

Santamouris, M., Haddad, S., Fiorito, F., Osmond, P., Ding, L., Prasad, D., Zhai, X., & Wang, R. (2017). Urban Heat Island and Overheating Characteristics in Sydney, Australia. An Analysis of Multiyear Measurements. Sustainability, 9(5), 712. https://doi.org/10.3390/su9050712

SMHI. (2021). Ladda ner meteorologiska observationer | SMHI. https://www.smhi.se/data/meteorologi/ladda-ner-meteorologiska-observationer#param=precipitationType24Hours,stations=all

SMHI. (n.d.). Hur var vädret? - Göteborg. https://www.smhi.se/klimat/klimatet-da-och-nu/hur-var-vadret/q/G%C3%B6teborg

Smoliak, B. V., Snyder, P. K., Twine, T. E., Mykleby, P. M., & Hertel, W. F. (2015). Dense Network Observations of the Twin Cities Canopy-Layer Urban Heat Island. Journal of Applied Meteorology and Climatology, 54(9), 1899–1917. https://doi.org/10.1175/JAMC-D-14-0239.1

Soltani, A., & Sharifi, E. (2017). Daily variation of urban heat island effect and its correlations to urban greenery: A case study of Adelaide. Frontiers of Architectural Research, 6(4), 529–538. https://doi.org/10.1016/j.foar.2017.08.001

Spronken-Smith, R. A., & Oke, T. R. (1998). The thermal regime of urban parks in two cities with different summer climates. International Journal of Remote Sensing, 19(11), 2085–2104. https://doi.org/10.1080/014311698214884

Spronken-Smith, R. A., & Oke, T. R. (1999). Scale Modelling of Nocturnal Cooling in Urban Parks. Boundary-Layer Meteorology, 93(2), 287–312. https://doi.org/10.1023/A:1002001408973

Stadsledningskontoret. (2022). Befolkningsprognos 2022–2040. Göteborgs Stad. https://goteborg.se/wps/wcm/connect/3f124c56-985b-4c45-8b6f-3fdd6f027c36/Kommunprognos+2021.pdf?MOD=AJPERES&CONVERT_TO=url&CACHEID=ROOTWORKSPACE-3f124c56-985b-4c45-8b6f-3fdd6f027c36-nw2IM0r

Statistiska Centralbyrån. (2022). Folkmängd i riket, län och kommuner 31 december 2021 och befolkningsförändringar 2021. Statistiska Centralbyrån. http://www.scb.se/hitta-statistik/statistik-efter-amne/befolkning/befolkningens-sammansattning/befolkningsstatistik/pong/tabell-och-diagram/helarsstatistik--

kommun-lan-och-riket/folkmangd-i-riket-lan-och-kommuner-31-december-2021-och-befolkningsforandringar-2021/

Taha, H. (1997). Urban climates and heat islands: Albedo, evapotranspiration, and anthropogenic heat. Energy and Buildings, 25(2), 99–103. https://doi.org/10.1016/S0378-7788(96)00999-1

Tam, B. Y., Gough, W. A., & Mohsin, T. (2015). The impact of urbanization and the urban heat island effect on day to day temperature variation. Urban Climate, 12, 1–10. https://doi.org/10.1016/j.uclim.2014.12.004

Thorsson, S., Lindberg, F., Björklund, J., Holmer, B., & Rayner, D. (2011). Potential changes in outdoor thermal comfort conditions in Gothenburg, Sweden due to climate change: The influence of urban geometry. International Journal of Climatology, 31(2), 324–335. https://doi.org/10.1002/joc.2231

van Hove, L. W. A., Jacobs, C. M. J., Heusinkveld, B. G., Elbers, J. A., van Driel, B. L., & Holtslag, A. A. M. (2015). Temporal and spatial variability of urban heat island and thermal comfort within the Rotterdam agglomeration. Building and Environment, 83, 91–103. https://doi.org/10.1016/j.buildenv.2014.08.029

Vilhelmson, B., & Elldér, E. (2021). Realizing proximity in times of deregulation and densification: Evaluating urban change from a welfare regime perspective. Journal of Transport Geography, 94, 103098. https://doi.org/10.1016/j.jtrangeo.2021.103098

Yang, J. H. (Joseph H. (2016). The curious case of urban heat island: A systems analysis [Thesis, Massachusetts Institute of Technology]. https://dspace.mit.edu/handle/1721.1/107347